EPJ Web of Conferences **52**, 01001 (2013)
DOI: 10.1051/epjconf/20135201001

The ATLAS Hadronic Physics Program and High Energy Cosmic Rays

J. L. Pinfold[1]

[1] Physics Department University of Alberta, Edmonton, Alberta T6G 0V1 Canada

Abstract. The various aspects of the current and future ATLAS programs to explore hadronic physics, including diffraction and forward physic are discussed The emphasis is placed on those results and future plans that have particular relevance for high-energy, and ultra high-energy, cosmic ray physics. In closing the latest ATLAS results on the search for the Higgs boson are summarized.

1 Introduction

The latest ATLAS results on the hadronic physics topics: the inelastic cross-section, the diffractive fraction, the charged particle multiplicity and the charged particle $P_{T,}$ are presented. These results have an important impact on our understanding of the physics of extended air showers of cosmic rays. Another key issue in this arena is the measurement of the total p-p cross-section that is the main physics goal of the ATLAS ALFA detector. A description of this detector along with the progress of the physics program is reported below. ATLAS is planning an important future upgrade project – ATLAS Forward Protons (AFP) - to deploy forward proton spectrometers initially at ±220m and finally, also at ±420m. A description of the detector and the status of AFP project is presented. Last, but definitely not least, the latest results on the newly discovered "Higgs boson-like" particle are very briefly summarized.

2 The ATLAS Detector

The ATLAS detector, shown in Figure 1 is described in detail elsewhere [1]. The LHC beam-pipe, runs along the cylindrical axis of the ATLAS detector. The ATLAS tracking detector, that encompasses the interaction point, uses silicon pixel, silicon strip, and straw tube technologies and is embedded in a 2 T magnetic field. The tracking system covers the pseudorapidity [2] range $|\eta| < 2.5$. It is surrounded by electromagnetic and hadronic calorimeters covering $|\eta| < 3.2$, which are complemented by a forward hadronic calorimeter covering $3.1 < |\eta| < 4.9$.

Minimum Bias Trigger Scintillator (MBTS) detectors, the primary detectors used in this measurement, are mounted in front of the endcap calorimeters on both sides of the interaction point at z = ±3.56 m and cover the range $2.09 < |\eta| < 3.84$. Each side consists of 16 independent counters divided into two rings; the inner 8 counters cover the rapidity range $2.83 < |\eta| < 3.84$ and the outer 8 counters cover the range $2.09 < |\eta| < 2.83$. Each individual counter spans 45° of the azimuthal angle (φ), and 31 out of 32 counters were operational. The luminosity is measured using a Cherenkov light detector, LUCID, which is located at z = ±17 m. The luminosity calibration has been determined during dedicated van der Meer beam scans to a precision of few percent [3, 4].

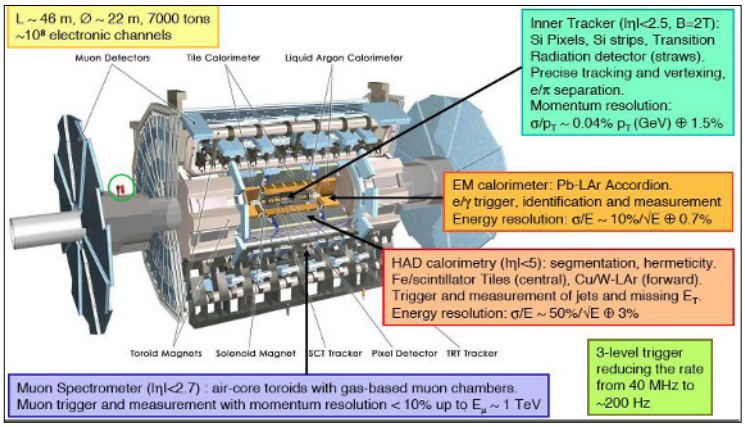

Fig. 1. A 3-D annotated depiction of the ATLAS detector at the LHC.

In the terms of pseudo-rapidity, the ATLAS detector can be divided into a central detector, which consists of an inner tracking detector ($|\eta|< 2.5$), a muon spectrometer ($|\eta| < 2.7$) and a calorimeter system ($|\eta|< 4.9$), and forward detectors which cover rapidities above. Currently, ATLAS is equipped with three forward detectors: LUCID, ZDC and ALFA. Zero Degree Calorimeter (ZDC) is placed at 140 m from the IP. It is situated at TAN region (target absorber for neutrals), which is the point where the single beam pipe splits into two [5]. ALFA (Absolute Luminosity for ATLAS) Roman Pots are situated at 240 m from the interaction point at both sides of the ATLAS. The Roman Pots system is able to move its scintillating fiber detectors close to beam [6]. The AFP (ATLAS Forward Proton) is a project aiming to install forward detectors at 220 m (AFP220) and 420 m (AFP420) around ATLAS for measurement of exclusive physics events – where the colliding protons doe not break up - at high luminosities [7].

3 The Inelastic Cross-section

The inelastic cross-section comprises all hadronic interactions that are not elastic. It corresponds to roughly 80% of the total hadronic cross-section. . The inelastic cross-section can be broken down into a diffractive (~30% of the inelastic cross-section) and non-diffractive component (~70% of the inelastic cross-section). The Non-diffractive collisions are due to parton-parton interactions - described by perturbative QCD. Diffractive events are due to colourless Pomeron exchange - described by Regge-Gribov type models. The main Feynman tree level diagrams that describe the inelastic cross-section process are given in Figure 2.

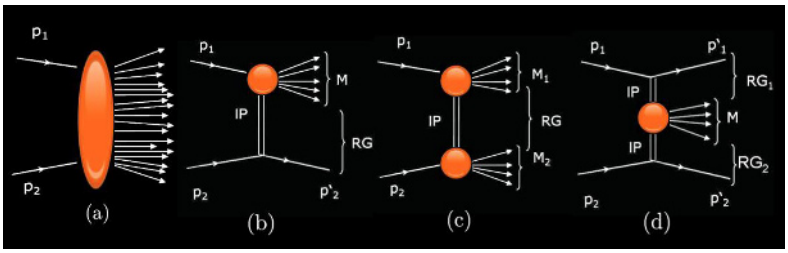

Fig. 2. Feynman diagrams for (a) non-diffractive events, (b) single diffractive events, (c) double diffractive events, (d) exclusive events.

In 2012 a first measurement of the inelastic cross-section for p-p collisions at a centre of mass energy $\sqrt{s}$ = 7 TeV, using the ATLAS detector at the Large Hadron Collider was reported [8]. In a dataset corresponding to an integrated luminosity of 20 μb^{-1}, events were selected by requiring hits on the MBTS scintillation counters mounted in the forward region of the detector. An inelastic cross-section of 60.3 ± 2.1 mb was measured for $\xi > 5 \times 10^{-6}$, where $\xi = M^2_X/s$ is calculated from the invariant mass, M_X, of hadrons selected using the largest rapidity gap in the event. For diffractive events this corresponds to at least one of the dissociation masses being larger than 15.7 GeV.

In Figure 3 the proton-proton cross-section from ATLAS and CMS is shown on the same plot as the inelastic cross-section estimated using the Glauber Model from the proton-air cross-section measured the Auger Collaboration [9]. We can see from this plot that the measurements are consistent with the growth of the inelastic cross-section predicted by the EPOS1.99 hadronic interaction model. Note also, that the inelastic cross-section is lower than predicted by all the other models. Thus, an energetic primary cosmic ray proton interacts deeper in the atmosphere than would have previously been expected, resulting in modified shower maximum distributions. The shower maximum is a key variable when it comes to assessing the composition of cosmic rays, for example with this slower rise in $\sigma_{inel.}$ the SIBYLL and QGSJET interpretations would move towards heavier elements at higher primary cosmic ray energies.

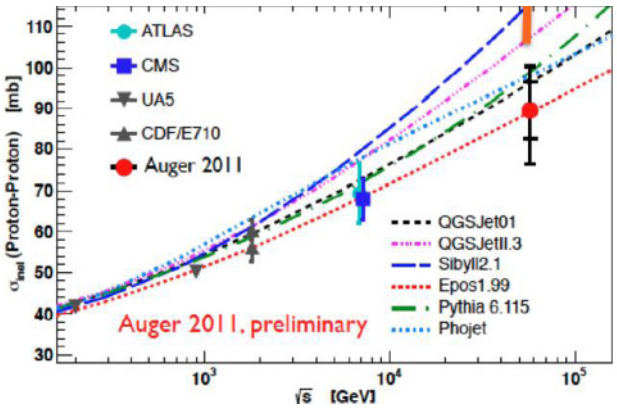

Fig. 3. A plot of the most recent proton-proton inelastic cross-section measurements made by the ATLAS, CMS, UA5, CDF/E710 and Auger experiments. In the case of the Auger measurement the inner error bars are statistical, while the outer include systematic uncertainties. The Auger measurement was derived from the proton-air cross-section using the Glauber formalism.

3.1 The Diffractive Fraction

The fractional contribution of diffractive events, f_D, is constrained by the ratio of single-sided to inclusive events, R_{SS}. The MC generators predict that less than 1% of the non-diffractive (ND) process pass the single-sided event selection, while 27 - 41% of the single diffractive (SD) and double diffractive (DD) processes pass the single-sided selection. For all models the inclusive sample is dominated by ND events, therefore the ratio of single-sided to inclusive events is sensitive to the relative fraction of diffractive events.

The measured R_{SS} in the data is R_{SS} = [10.02 ± 0.03(stat.) +0.1 −0.4(syst.)]%, where the systematic error includes the uncertainties on the backgrounds, the MBTS response and the material. Figure 4 contrasts the observed value of R_{SS} to the predictions of several models as a function of f_D. The intersection of the R_{SS} value measured in data with the prediction is used as the central value of f_D for each model. The systematic uncertainty on f_D is determined by the maximum and minimum values consistent with the 1σ uncertainty on the data when varying the double- to single dissociation event ratio between 0 and 1. The resulting value using the default Donnachie and Landshoff (DL) model [10], model is f_D = 26.9+2.5 −1.0%.

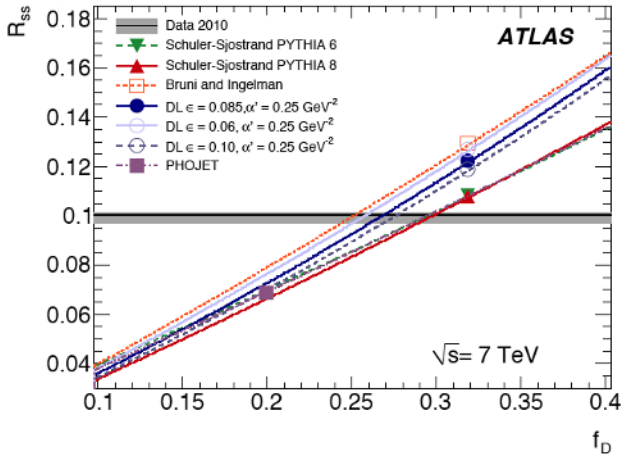

Fig. 4. The ratio of the single-sided to inclusive event sample R_{SS} as a function of the fractional contribution of diffractive events to the inelastic cross-section f_D. The data value for R_{SS} is shown as the horizontal line with its systematic uncertainties (grey band). Also shown are predictions of several models as a function of an assumed value of f_D. The default f_D value (32.2% for all models but Phojet which is 20.2%) is indicated by the markers.

4 Charged Particle Multiplicities

The ATLAS detector at the LHC was used to make measurements of proton-proton collisions at centre-of-mass energies of $\sqrt{s}$ = 0.9, 2.36 and 7 TeV [11]. Events were collected using a single-arm minimum-bias trigger. The charged-particle multiplicity, its dependence on transverse momentum and pseudorapidity and the relationship between the mean transverse momentum and charged-particle multiplicity were measured. Measurements in different regions of phase-space are shown, providing diffraction-reduced measurements as well as more inclusive ones. The observed distributions are corrected to well-defined phase-space regions, using model-independent corrections. The results are compared to each other and to various Monte Carlo models, including a new AMBT1 Pythia6 tune.

Events in which the Inner Detector was fully operational and the solenoid magnet was on are used for this analysis for both $\sqrt{s}$ = 0.9 TeV and $\sqrt{s}$ = 7 TeV. During this data taking period, more than 97% of the Pixel detector, 99% of the SCT and 98% of the TRT were operational. At $\sqrt{s}$ = 2.36 TeV the requirements are the same, except for the SCT being in standby. Events were selected from colliding proton bunches in which the MBTS trigger recorded one or more counters above threshold on either side. The maximum instantaneous luminosity is approximately 1.9 x 10^{27} cm^{-2} s^{-1} at 7 TeV. The probability of additional interactions in the same bunch crossing is estimated to be of the order of 0.1%.

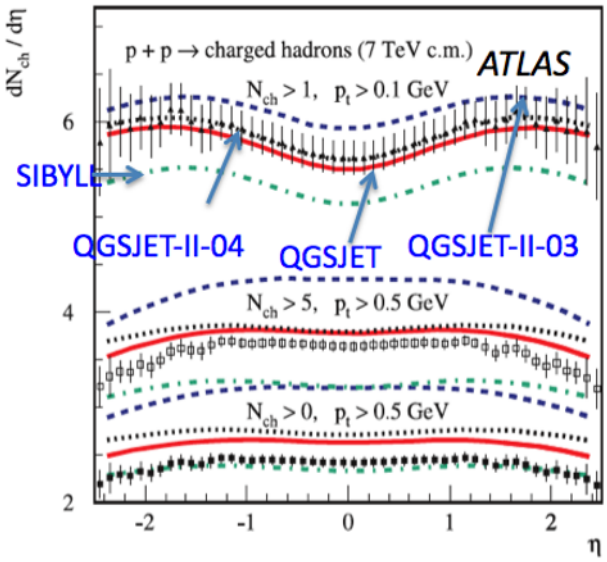

Fig. 5. Charged-particle multiplicity distributions for events with n_{ch} >0,1,5, p_T > 0.1/0.5 GeV & $\sqrt{s}$ = 7 TeV.

Inclusive charged-particle distributions have been previously measured in p.p and p.pbar collisions at a range of different centre-of-mass energies [11]. These measurements provide insight into the strong interactions at low energy-scales. Several QCD-inspired models have been developed to interpret them. These models are frequently cast into Monte Carlo simulations with free parameters that can be constrained by measurements such as minimum bias distributions. These measurements contribute to the understanding of soft QCD; moreover, they are important to determination of biases on high-pT phenomena due to underlying events and event pileup effects and are therefore of growing importance for future LHC physics.

In all the kinematic regions considered, the particle multiplicities are higher than predicted by the Monte Carlo models. The central charged-particle multiplicity per event and unit of pseudorapidity, for tracks with p_T > 100 MeV, is measured to be 3.483 ± 0.009 (stat) ± 0.106 (syst) at $\sqrt{s}$ = 0.9 TeV and 5.630 ± 0.003 (stat) ± 0.169 (syst) at $\sqrt{s}$ = 7 TeV. As can be seen in Figure 5 it turns out that the predictions of various hadronic models bracket ATLAS data on particle multiplicity. The LHC centre-of-mass energy of 7 TeV is equivalent to a cosmic ray proton of energy 3 x 10^6 eV in the Knee region of the cosmic ray energy spectrum. Thus, ATLAS results indicate that new physics scenarios for the knee are unlikely.

4.1 Energy Evolution of the Particle Density

Figure 6 shows the mean track multiplicity at central rapidity for all centre-of-mass energies and phase-space regions presented in this paper, along with predictions from Pythia6 AMBT1 tune. As can be seen the minimum bias mid-η energy evolution is strongly model dependent. Extrapolations to the UHE GZK cutoff region: $E_{cm} \sim 40$ x E_{cm}(LHC) show large uncertainties.

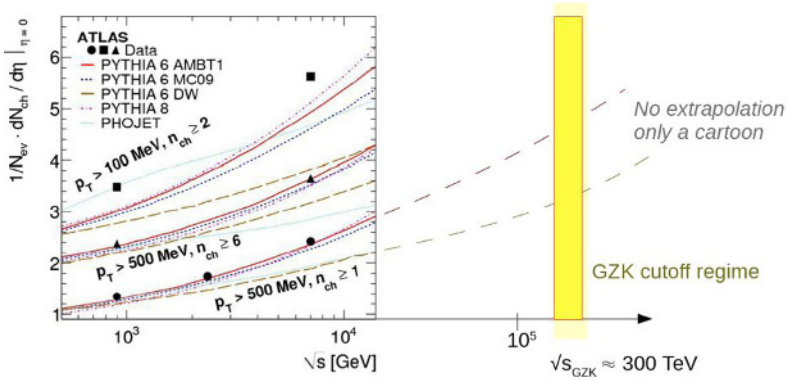

Fig. 6. The average charged particle multiplicity per unit of rapidity for η = 0 as a function of the centre-of-mass energy. All the measured phase-space regions and energies are shown as triangles and compared to predictions from Pythia6 AMBT1 tune. The phase-space region label is above the corresponding curves and points.

4.2 Transverse Energy Density and the Average Transverse Momentum

Figure 7 shows the evolution of the transverse energy density with p_T as well as the average p_T as a function of charge particle multiplicity. These distributions and others reported in Ref. [11] show that the simulations generally predict a harder spectrum for $p_T >$ ~ GeV/c and also that the average predicted p_T is larger than that of the data.

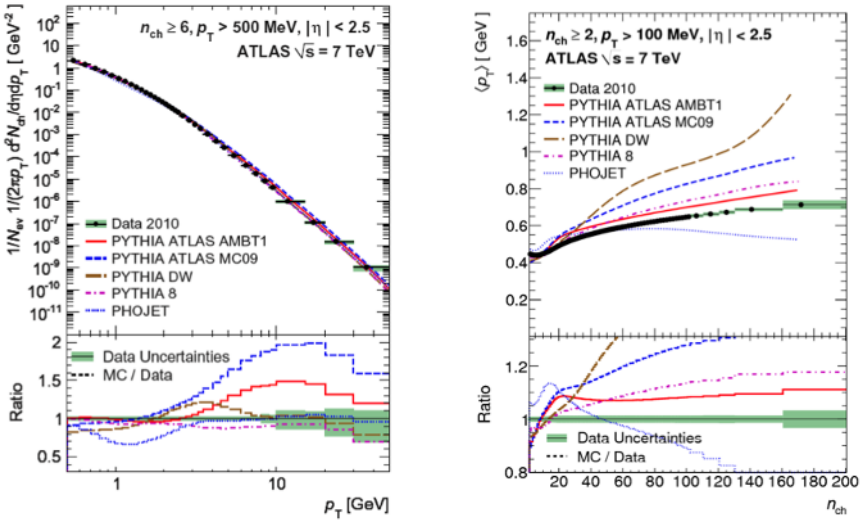

Fig. 7. (Left) Charged-particle multiplicities as a function of the transverse momentum for events with $n_{ch} \geq 6$, $p_T > 500$ MeV and $|\eta| < 2.5$ at $\sqrt{s} = 7$ TeV. The dots represent the data and the curves the predictions from different MC models. The vertical bars represent the statistical uncertainties, while the shaded areas show statistical and systematic uncertainties added in quadrature. The bottom inserts show the ratio of the MC over the data. The values of the ratio histograms refer to the bin centroids. (Right) Average transverse momentum as a function of the number of charged particles in the event for events with $n_{ch} \geq 2$, $p_T > 100$ MeV and $|\eta| < 2.5$ at $\sqrt{s} = 7$ TeV.

5 The ALFA Detector Project

ALFA (Absolute Luminosity for ATLAS) Roman Pots are situated at ~ ±240m from the ATLAS interaction point. The purpose of the Roman Pot system is to move ALFA's scintillating fibre detectors close to beam [12]. At beginning of the run the ALFA detectors are in withdrawn position far from the beam. When the beam is stabilized the detectors are inserted to the measurement position. ALFA detectors are primarily intended to make an absolute luminosity measurement and determine the elastic pp cross section. ALFA will collect data in special LHC run with high β^* optics. The precision of the luminosity measurement is expected to be ~2-3%. Apart from the elastic processes, ALFA plans to study soft diffraction processes at low luminosity.

In diffractive processes one or both protons survive the collisions and are slightly deflected from the original direction. The intact proton then propagates through

magnetic field of the LHC magnets and remains in beam pipe. Such proton can be detected in the Roman Pots. The cross section of the diffraction processes is described as a function of the fractional momentum lost ξ and the momentum transfer $t = (p_i - p)^2 \sim -p_T^2$ where p_i is four-momentum of incoming proton, p and p_T is four-momentum and transverse momentum of the scattered proton respectively. The variables ξ and t are computed from the proton momentum angle and position reconstructed in Roman Pots. The ALFA is able to measure ξ in interval 0.01 to 0.1 with accuracy of 8% to ~ 2% respectively.

The principle of luminosity L determination then lies in the fitting of the measured distribution to a form motivated by the proton-proton (pp) differential cross section (see Figure 8) assuming that we can write the fit, in the considered kinematic region, in the form: $dN_{el}/dt = L|A_C + A_N|^2$, where dN_{el}/dt is the number of elastically scattered protons with 3-momentum p through an angle θ per second, $|t| \sim (p\theta)^2$. $A_{C,N}$ corresponds to the electromagnetic (Coulomb), respectively strong (Nuclear), amplitude and σ_{el} the total elastic cross section for the pp interaction.

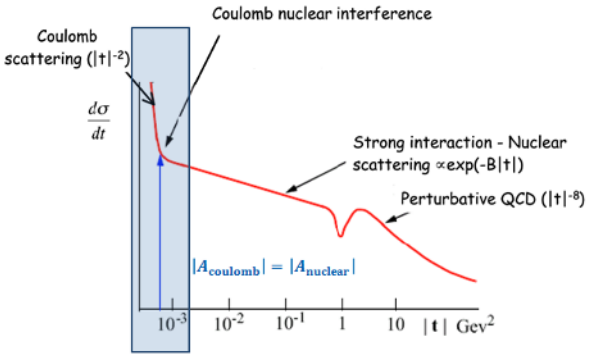

Fig. 8. Elastic pp differential cross section.

5.1 The ALFA Physics Program

It is quite a challenging task to reach the Coulomb region (see Fig. 8) as detectors must be moved close to the beam (~1.5 mm). If, from some reason, it is not possible to reach the Coulomb region we can still determine the luminosity and the total cross section. With the help of the optical theorem we can write: $L = (1/16\pi)[N_{tot}(1 + \rho^2)]/[dN_{el}/dt|_{t=0}]$ and $\sigma_{tot} = [16\pi/(1 + \rho^2)][dN_{el}/dt|_{t=0}/N_{tot}]$ where ρ is the ratio of the real and imaginary parts of elastic scattering amplitude and $N_{el(tot)}$ is the elastic (total) rate.

The data at small values of t has to be corrected for the detector acceptance using a Monte Carlo simulation and N_{tot} has to be determined via a measurement. There is a possibility to use e.g. the Minimum Bias Trigger Scintillators (MBTS) detector. Its efficiency is different for each component of the total cross section $\sigma_{tot} = \sigma_{el} + \sigma_{SD} + \sigma_{DD} + \sigma_{ND}$. Based on PYTHIA 6.4 simulations the efficiencies are 68% for single diffractive (SD), 82% for the double diffractive (DD) and 100% for the non-diffractive (ND) component (E_{beam} = 7TeV).

The detector system ALFA is installed and functioning. The measurement of the absolute luminosity together with the determination of the pp total cross-section and the parameters ρ and the nuclear slope (B) represents the first priority for the ALFA detector. The plan for the future is as follows: 2011-2013: determine the t-spectrum and total cross section measurements with precision < 5% at the centre-of-mass-energy of 7-8 TeV; 2014 onwards, determine the luminosity and total cross section measurements at the centre-of- mass energy of 14 TeV.

Beyond the main physics program there are at least two other potential regions of interest where the ALFA detector can contribute. Simulations show that ALFA has a potential to detect protons from soft single diffractive dissociation processes. The ALFA detector can also measure exclusive processes - where the beam protons interact but do not break up - like pp→ ppπ+π−.

6 The AFP Project

The primary goal of the ATLAS Forward Proton (AFP) project [13] is to enhance the diffractive physics programme of the ATLAS experiment by installing new detectors that will be able to tag forward protons scattered at very small angles. This will allow us to use the LHC not only as p-p collider but also as a pomeron-pomeron, photon-photon and photon-pomeron collider – enabling us to study Single Diffraction, Double Pomeron Exchange, Central Exclusive Production and photon-photon processes.

The AFP (ATLAS Forward Proton) project aims to initially i.e during Phase-0/1 envisaged to start around 2016/19, to install forward proton spectrometers at ±206m & ±214m on either side of the ATLAS interaction point. In Phase-2 detectors will be added at ±420 m. In the first station at 206m, in one pocket of a moveable beam-pipe, a tracking station composed by 6 layers of Silicon detectors will be deployed. The second station at 214m will contain another tracking station and a timing detector - this setup is mirrored on the opposite side of the ATLAS IP.

The key requirements for the silicon tracking system at 220 m are spatial resolution of ~10 (30) μm per detector station in x (y) and angular resolution for a pair of detectors of about 1 μrad. High efficiency is needed over the area of 20 x 20 mm^2 corresponding to the distribution of diffracted

protons and minimal dead space at the edge of the sensors allowing scattered protons at low angles to be measured. The tracking detectors must have sufficient radiation hardness to sustain the radiation at high luminosity and be capable of robust and reliable operation at high LHC luminosity.

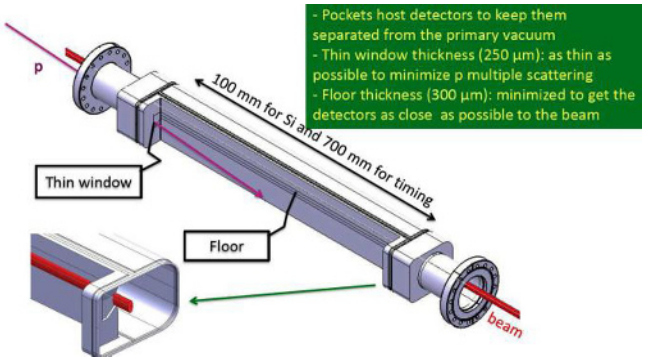

Fig. 9. The moveable beam-pipe (Hamburg pipe) scheme for deploying detectors near to the beam.

The tracker when combined with the LHC dipole and quadrupole magnets, forms a powerful momentum spectrometer with which to measure protons emerging intact from the pp interactions so allowing ATLAS to exploit the program of exclusive physics (where the interacting protons do not breakup) at the LHC. The two main physics motivations of the ATLAS Forward Physics Project are the study of the anomalous couplings between photons and W or Z boson and the measurement of diffractive Higgs production at the LHC

The idea of movable "Hamburg" beam pipes is simple, a larger section of the LHC beam pipe than usual can move close to the beam using bellows so that the detectors located at its edge (called pocket) can move within a few millimeters from the beam when the beam is stable (during injection, the detectors are in parking position). A basic sketch of this system is given in Figure 9 above.

A fast timing system that can precisely measure the time difference between outgoing scattered protons is a key component of the AFP detector. The time difference is equivalent to a constraint on the event vertex, thus the AFP timing detector can be used to reject overlap background by establishing that the two scattered protons did not originate from the same vertex as the central system. The final timing system should have a 10 ps or better resolution (giving a factor 40 rejection on pile up background). The efficiency must be close to 100% over the detector acceptance and a high rate capability is required (there is a bunch crossing every 25 ns at the nominal LHC). Last, but not least sufficient segmentation is needed for multi-proton timing Level-1 trigger capability

With detectors at ~ ±220m this device is sensitive to diffractive masses in the ATLAS detectors between 350 GeV and 1.4 TeV. The advantage of this apparatus from the physics point of view is that the system is fully constrained: we measure all the particles in the final state, namely the two intact protons and the particle produced (W, Z, the Higgs boson or the SUSY particles). The mass and the kinematical properties of the produced particles are computed using the tagged proton information.

7 Latest Results on the Discovery of a New "Higgs-Like" Particle

The latest results on the continuing study of the new " Higgs-like" particle the discovery of which was announced on July 4th 2012 [14] are summarized in Figure 10. The signal strength plot (left), where signal strength is $\sigma_{meas.}/\sigma_{SM}$ indicates that the measured cross-sections, except perhaps that of H→γγ, are all consistent with the SM. The right hand plot shows that the significance of the combined channels shows that the new particle signal is now well above the significance of 5σ that conventionally marks the threshold significance necessary to claim discovery.

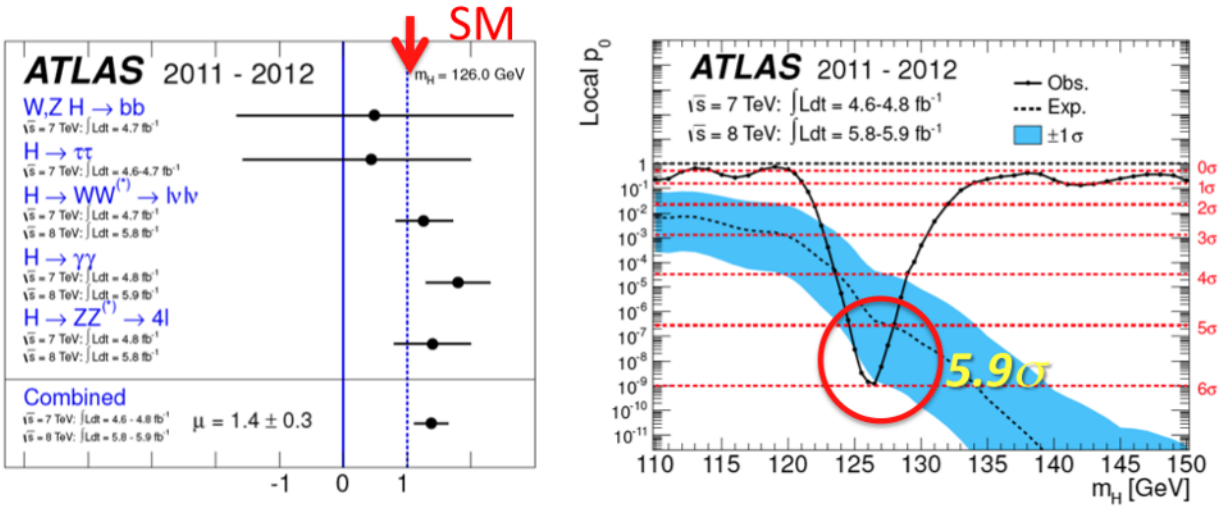

Fig. 10. (Left) Signal strength of new particle production for the various decay modes studied. (Right) The significance of the combined result.

8 Conclusions and the Future

The hadronic physics results from ATLAS show that a less than perfect agreement with the various standard Monte Carlo models used in the particle and astroparticle physics arenas. However, these models are still broadly descriptive of the observed ATLAS hadronic physics program data. The ATLAS data recorded over the last year or so were taken at a centre-of-mass energy that is equivalent to a cosmic ray proton energy 10^{17} eV slightly beyond the knee region (~10^{16} eV). Consequently, we can rule out the hypothesis that the knee in the cosmic ray spectrum is due to the presence of some strong indication of new hadronic physics threshold, where some 20% of the cosmic ray primary energy would need to be transferred to invisible channels, since ATLAS did not see evidence for this.

The hadronic results from the LHC detectors are useful in refining the models used in high-energy air shower physics reducing the required extrapolation factors to a factor of ~40. ATLAS data indicates a slower energy rise of the inelastic cross-section than was predicted by a number of models. This leads to a reduction in the p-Air cross-section and on average a deeper extended air shower maximum position resulting in a move towards heavier elements as the cosmic ray primary energy increases. Also the measurement of the inelastic p-N - and subsequent estimate of the p-p cross-section – was a useful result in assessing various hadronic models at LHC energies. Indeed, it seems that some models, for example EPOS 1.99, normally utilized largely for studies of cosmic ray air showers, are proving to be a valuable complement to the models traditionally used for studies at LHC energies.

The future physics program of ATLAS should enhance to the synergy between cosmic ray and collider physics. The results from ALFA on the elastic p-p cross-section will be published in the coming months. The LHC had a period of p-N running this year (although p-Pb not nitrogen!) that is expected to soon yield results of interest to the cosmic ray community. Another important recent development in this area is the creation of an official ATLAS "Astroparticle Physics Forum". Last, but not least, starting in 2015 after the long shutdown The LHC will be running at a entre-of-mass energy of 14 TeV. This will enable us to test our hadronic models in a new energy regime and reduce the extrapolations of LHC results required to study very high energy extended air shower physics.

References

1. ATLAS Collaboration, JINST 3 (2008) S08003.
2. ATLAS uses a right-handed coordinate system with its origin at the nominal interaction point (IP) in the centre of the detector and the z-axis coinciding with the axis of the beam pipe. The x-axis points from the IP to the centre of the LHC ring, and the y axis points upward. Cylindrical coordinates (r, f) are used in the transverse plane, f being the azimuthal angle around the beam pipe. The pseudorapidity is defined in terms of the polar angle q as h = −ln tan(q/2).
3. S. van der Meer, CERN-ISR-PO-68-31, 1968.
4. ATLAS Collaboration, ATLAS-CONF-2011-011;
5. ATLAS Zero Degree Calorimeters for ATLAS, ATLAS Collaboration, Letter of Intent, December 1 2007, http://cdsweb.cern.ch/record/1009649
6. ATLAS Collaboration, ATLAS Forward Detectors for Measurement of Elastic Scattering and Luminosity, TDR, January 17, 2008 http://atlas-project-lumi-fphys.web.cern.ch/atlas-project-lumi-fphys/tdr.pdf
7. http://atlas-project-lumi-fphys.web.cern.ch/atlas-project-lumi-fphys.
8. G. Aad et al., ATLAS Collaboration, Nature Commun. 2 (2011) 463
9. P. Abreu et al., Pierre Auger Collaboration, FERMILAB-PUB-11-489-AD-AE-CD-TD, 8 pages (2011).
10. A. Donnachie and P. V. Landshoff, Nucl. Phys. B244, (1984) 322.
11. G. Aad et al., The ATLAS Collaboration, New Journal of Physics 13, 053033 (2011).
12. T. Sykora, For the ATLAS Collaboration, ATL-PHYS-PROC-2011-250 (2011), S. Jakobsen et al., ATLAS ALFA Collaboration, Nucl. Instr. Meth. A695, 342-346 (2012).
13. R. Staszewski, For the ATLAS AFP Group, Acta Phys.Polon. B42, 1615-1624 (2011).
14. G. Aad et al., ATLAS Collaboration, Phys. Lett. B716, 1-29 (2012).